Prediction of Pull-Out Performance of Chemical Anchors Embedded into Concrete

Ilker Bekir Topcu[1], , Mucteba Uysal[2], Harun Tanyildizi[3]

[1]Eskisehir Osmangazi University, Department of Civil Engineering, Eskisehir, Turkey

[2]Sakarya University, Department of Civil Engineering, Sakarya, Turkey

[3]Firat University, Department of Civil Engineering, Elazig, Turkey

Abstract

This paper summarizes the results of experimental research and prediction model focused on determination of the behavior of pull-out performance limits of what embedded into currently the most widespread concrete type of Turkey as C25/30. Rebars having 14, 16 and 18 mm diameters have been selected as the anchor rod in this study. Epoxy based three component chemical adhesive has been used for the connection between concrete and anchor bar. The depth of holes was in the range of 140 - 220 mm which had been selected various for 14, 16 and 18 mm bar diameters. The effect of the anchor depths, bar diameters and reinforcement diameter on the pull-out capacity of adhesive anchors is product dependent. Moreover, an attempt to predict the pull-out capacity of chemical anchors embedded into concrete using artificial neural networks (ANNs) is presented. The problem is proposed to network models by means of three inputs and one output parameter. A multilayered feed-forward neural network trained with the different algorithm is constructed using 3 design variables as network inputs and the pull-out strength of adhesive anchors as the only output. Experimental results showed that increasing the anchor diameter and the depths of hole have increased pull-out performance of anchors. The best algorithm for collapse load of concrete is the Levenberg-Marquardt backpropagation with R^2 of 0.9837. The results indicated that ANNs are useful technique for predicting the pull-out capacity of adhesive anchors.

Keywords: Anchor; pull-out performance; rebar diameter; depths of holes; artificial neural networks.

1. Introduction

The researches and applications of an anchor embedded in a hardened cementitious material such as concrete have been carried out for many decades. For the convenience of the anchors embedded more efficiently in the concrete, researchers began to adopt post-installation for bonding the reinforcements into the concrete. General operations are drilling a hole in hardened concrete and installing a steel rod into the concrete with adhesive or cement grout.

Chemical anchors are also getting more frequently used to connect structural elements. Anchors that are used to provide the connection between two different elements can be categorized under two categories as cast-in-place and post-installed anchorages. Post-installed anchorages could be manufactured using different methods such as mechanical, grout or chemical. Recently, more researches have focused on adhesive bonded anchors [1-3]. The variables investigated included the condition of the drilled hole, concrete compressive strength, aggregate type, adhesive curing period and loading at elevated temperature. Cook et al. analyzed the behaviors of single adhesive anchors and single headed or unheaded grouted anchors under tensile load in concrete [4-6]. General failure modes of these anchorage systems can be summarized as pullout of a concrete cone, debonding at anchor–adhesive/grout or concrete–adhesive/grout interface, fracture of anchor, and combination of some of these failure modes. Then several design models were recommended taking into account of all the possible failure modes. Moreover, for an adhesive anchor installed into a damp, wet and uncleaned hole, the bond strength between anchor and concrete was generally reduced [7]. An adhesive anchor is installed using a rebar or threaded rod inserted in a drilled hole in hardened concrete using a polymer-based bonding agent including epoxies, vinylesters and polyesters. Typically, a grouted anchor isa threaded rod, headed bolt or deformed rebar inserted in a drilled hole filled with a cementitious or polymer grout. In this case, the diameter of the predrilled hole is at least 150% larger than that of the fastener [8].

The bond strength of rebars is a function of the geometric and material properties of the concrete member and the rebars. Several factors influence the pull-out performance of anhors. The most important of them are concrete compressive strength, splice length, the relative rib area (the ratio of projected rib area normal to bar axis to the product of the nominal bar perimeter and the center-to-center rib spacing), minimum concrete cover defined as the smallest of clear concrete covers in bottom and/or sides or 12 of the clear spacing between bars, the amount of transverse steel area to spacing ratio and the splice bar size illustrated as ratio of the area of the splice bar to the effective cross section of the beam [9]. Tepfers [10] illustrated that the bond

strength increases as cover and bar spacing increase. The mode of failure also depends on cover and bar spacing. For large cover and bar spacing, it is possible to obtain a pull-out failure, but for smaller ones, a splitting tensile failure occurs resulting in lower bond strength.

The approach based on the assumption of separated failure modes generally defines the resistance of an anchor for three load-bearing capacity values. As shown in Fig. 1a, the first failure mode is the tensile failure of the steel anchor element. This failure is clearly defined by the area of the shank of the rebar. The second failure mode is defined as a full concrete failure. This failure typically takes the form of a breakout cone (Fig. 1b). It is usually described as being dependent on concrete strength and the anchorage length. The third failure mode is the extraction of the rebar from the concrete. This can occur via the failure of the concrete–glue interface, the glue–steel interface or via the failure of the glue itself (Fig. 1c). Usually in design methods, the definition of the pull-out resistance for this failure type is related to one of the surfaces of the interface. This is possible because the thickness of the glue layer is small (several millimetres). This failure mode is termed ‘bond failure.

Fig. 1. Separated failure modes used in design methods: (a) tensile failure of the steel anchor bolt, (b) full concrete failure, and (c) bond failure: extraction of the steel bolt from the concrete [11].

Their main function is to transfer normal loads (tension and compression) and possible shear loads according to efforts at the base of the structure. The three main anchoring systems are the straight rod, the hooked rod and the headed rod. The tensile load is transferred through a bond between the steel rod and the concrete and/or abutment of the anchor plate or the hook on concrete. Load capacities of the mechanisms depend on the type and dimensions of anchor used. Under tension, the three main failure mechanisms are the breaking of the rod, the sliding of the rod and cone-shaped concrete breakout [12].

The artificial neural networks solve very complex problems with the help of interconnected computing elements. Basically, the processing elements of a neural network are similar to the neurons in the brain, which consist of many simple computational elements arranged in layers. In recent years, the ANNs and other models have been extended extensively and applied to many civil engineering applications such as epoxy-adhesive anchor systems. Similar results were also found in the experimental and numerical simulation studies by Li et al. [13]. James

et al. developed an approximate expression to predict the ultimate tensile capacity of the epoxy-adhesive anchors based on the analysis of linear and nonlinear finite element method [14]. Bickel and Shaikh utilized two methods with proper adjustments to predict the shear capacity of single adhesive anchors [15]. Sakla and Ashour introduced artificial neural networks into predicting the tensile capacity of single adhesive anchors and found that the tensile capacity is linearly proportional to the embedment length [8]. Moreover, Beard and Lowe [16] adopted the ultrasonic guided waves to successfully inspect the maximum anchor length for a grouted anchor.

The aim of this study is the investigation of that increasing the anchor diameter and the depths of hole on the performance of pull-out what embedded into currently the most widespread concrete type of Turkey. Furthermore, ANN model is constructed to predict the pull-out performance of chemical anchors embedded into concrete.

2. Experimental study

To measure the ultimate load for each anchor, a pullout test was performed to the specimens. Many strengthening applications are performed on buildings that are made of widespread concrete strength type of a country in order to better represent the practice, the anchors have been embedded in concrete elements. Preliminary data indicated that most concrete existing in Turkey has a compressive strength of 25 MPa for 15x15x15 cm cubic specimens and anchors were embedded in the concrete in scope of the study. Other parameters that have been used in this study are the anchor bar diameter and the anchor depth. In this study, rebars of three different diameters, namely 14, 16 and 18 mm have been embedded in depths that are 140, 150, 160, 170, 180, 190, 200, 210 and 220 mm as can be seen in Table 1. A total of 30 test specimens have been produced. Each data point represents the average of five measurements. The manufactured test specimens have been cured under laboratory conditions. Following this, the holes where the anchor bars will be embedded have been drilled. The holes were cleaned by using pressurized air from an oil-free compressor. The anchor bars have been embedded in the concrete blocks using epoxy resin and necessary precautions have been taken in order to the bars not to move until the epoxy has gained strength. The embedded anchors were covered by a loading block. Testing procedure can be seen in Fig.2a-b-c.

Table 1. Anchor depth, anchor diameter and rebar diameter of the specimens.

Fig.2. (a) Drilling, (b) cleaning and (c) embedding of the rebar specimens.

Pattex CF 900 Epoxy was used in this study. Mix proportions and mechanical properties of the epoxy are listed in Table 2.

Table 2. Mechanical properties and mix proportions and of the epoxy.

After emmedding rebar specimens on the curtain wall the bar specimens have been loaded by a hydraulic test apparatus on the curtain wall. Fig.3 shows pull-out of anchor rebar hydraulic test apparatus.

Fig.3. Hydraulic test apparatus of anchor rebar.

3. Test results

Fig. 4, Fig. 5 and Fig.6 show the results obtained from the anchor pull-out measurements of all the specimens emmebbed into concrete. It is shown in the Fig. 4 that the rebar of 14 mm of diameter has various embedment depths in the range of 140-180 mm. The pull-out strength capacity has been observed to increase with increasing diameters as it was expected. However, with increasing embedment depth, a significant change could be observed in capacity of the specimens. Pull-out strength of the specimens increases with an increasing the depths of hole and there is a notable reduction in pull-out strength of the specimens when embedment diameter decrease from 22 mm to 20 mm. The rebar specimen has 14 mm diameter and 180 mm embedment depth showed pull-out strength performance 18.54 % more than 150 mm embedment depth. Caliskan et al. investigated shear strength of epoxy anchors embedded into low strength concrete and found similar test results [3].

.

Fig.4. Test results of pull-out strength of the specimens have 14 mm rebar diameter.

Fig. 5 shows that the rebar of 16 mm of diameter has various embedment depths in the range of 160-200 mm. The pull-out strength capacity has been observed to increase with increasing diameters. However, with increasing embedment depth, a significant change could be observed in capacity of the specimens. Pull-out strength of the specimens increases with an increasing

the embedment depth and there is a notable reduction in pull-out strength of the specimens when embedment diameter decrease from 24 mm to 22 mm. The rebar specimen has 16 mm diameter and 200 mm embedment depth showed pull-out strength performance 18.37 % more than 160 mm embedment depth. Xu et al. modelled of anchor bolt pullout in concrete based on a heterogeneous assumption in this context made tests for influence of the embedded depth on the peak pullout load and found similar test results [17]. It can be seen in that research with the increase of the embedded length, the peak pullout load increases.

Fig.5. Test results of pull-out strength of the specimens have 16 mm rebar diameter.

Fig.6. Test results of pull-out strength of the specimens have 18 mm rebar diameter.

Fig. 6 shows that the rebar of 18 mm of diameter has various embedment depths in the range of 180-220 mm. Pull-out strength of the specimens increases with an increasing the embedment depth and there is a notable reduction in pull-out strength of the specimens when embedment diameter decrease from 26 mm to 24 mm. The rebar specimen has 18 mm diameter and 220 mm embedment depth showed pull-out strength performance 11.69 % more than 180 mm embedment depth.

4. Artificial neural network model for prediction of experimental results

ANN can exhibit a surprising number of human brain characteristics [18-26]. The fundamental concept of neural networks is the structure of the information processing system [27, 28]. They are consisting of a large number of simple processing elements called as neurons. A schematic diagram for an artificial neuron model is given in Fig. 7.

Fig. 7. Artificial neuron model.

Let $X=(X_1, X_2 \ldots X_n)$ represent the n input applied to the neuron. Where W_j represents the weight for input X_j and b is a bias, then the output of the neuron is given by Eq. 1. These neurons are connected with connection link. Each link has a weight that is multiplied by transmitted signal in network. Each neuron has an activation function to determine the output. There are many kinds of activation functions. Usually nonlinear activation functions such as sigmoid, step are used. ANNs are trained by experience, when an unknown input is applied to the network it can generalize from past experiences and produce a new result [29-32].

$$u = \sum_{j=0}^{m} x_j w_j - b \text{ and } V = f(u) \quad (1)$$

Artifical neural networks are systems that are deliberately constructed to make use of some organizational principles resembling those of the human brain [29-32]. They represent the promising new generation of information processing systems.

When designing an ANN model, a number of considerations must be taken into account. At first the suitable structure of the ANN model must be chosen. Then, the activation function need to be determined. The number of layers and the number of units in each layer must be chosen. Generally desired model consists of a number of layers. The most general model assumes complete interconnections between all units. These connections can be bidirectional or unidirectional. ANN can create its own organization or representation of the information it receives during learning time [28-33]. There are many kind of ANN structure. One of these is multilayer feed forward ANN and is shown in Fig. 8.

Fig. 8. Multilayer feed forward neural network structure.

In this study, the problem is proposed to network models by means of three inputs and one output parameter. The parameters such as reinforcement diameter, anchor depth, anchor diameter were selected as input variables. The model output variables were the collapse load. A data set including 30 data specimens obtained from experimental studies were used for artificial neural networks. The data were normalized by dividing with max values. ANN architecture used for this study is given in Fig. 9.

Fig. 9. ANN architecture.

Some ANN algorithms were used just learning in this study such as the BFGS Quasi-Newton backpropagation, the Powell-Beale Conjugate gradient backpropagation, the Fletcher-Powell conjugate gradient backpropagation, the Levenberg-Marquardt backpropagation, the One Step Secant backpropagation, the Resilient backpropagation, the Scaled conjugate gradient backpropagation. The computer program was performed under MATLAB software using the neural network toolbox. In the training, the number of neuron on the hidden layer changed to find best results. The best result for the BFGS quasi-Newton backpropagation was obtained from the seventeen neurons. The best result for the Powell-Beale conjugate gradient backpropagation algorithm was obtained from the eight neurons. The best result for the Fletcher-Powell conjugate gradient backpropagation was obtained from the eleven neurons.

The best result for the Levenberg-Marquardt backpropagation was obtained from the five neurons. The best result for the One step secant backpropagation was obtained from the eighteen neurons. The best result for the Resilient backpropagation was obtained from the twenty-three neurons. The best result for the Scaled conjugate gradient backpropagation was obtained from the fourteen neurons. A data set including 30 data specimens obtained from experimental studies were used for artificial neural networks. From these, 15 data patterns were used for training the network, and the remaining 15 patterns were randomly selected and used as the test data set. Fig. 10-16 present the measured collapse load and the predicted collapse loads by ANN model with R^2 coefficients. As it is visible in Figs. 10-23, the values obtained from the ANN models are very close to the experimental results. Furthermore, All of R^2 values show that the proposed ANN models are suitable and can predict collapse load of concrete of the experimental values. This can be also observed in the other articles related to predicting concrete properties [26-29]. Fig.12 shows that the best algorithm for collapse load of concrete is the Levenberg-Marquardt backpropagation with R^2 of 0.9837. The training performance during the training process is given in Fig. 17-23 where the variation of mean-square error with training epochs is illustrated. Artificial neural networks are capable of learning and modeling using the data obtained from experiments. This makes artificial neural networks a powerful tool for solving some of the complicated civil engineering problems [33].

Figure 10. Linear relationship between measured and predicted compressive strengths for the BFGS quasi-Newton backpropagation.

Figure 11. Linear relationship between measured and predicted splitting tensile strengths for the Powell-Beale conjugate gradient backpropagation.

Fig. 12. Linear relationship between measured and predicted compressive strengths for the Levenberg-Marquardt backpropagation.

Figure 13. Linear relationship between measured and predicted compressive strengths for the Fletcher-Powell conjugate gradient backpropagation.

Fig. 14. Linear relationship between measured and predicted splitting tensile strengths for the One step secant backpropagation.

Figure 15. Linear relationship between measured and predicted splitting tensile strengths for the Resilient backpropagation.

Figure 16. Linear relationship between measured and predicted compressive strengths for the Scaled conjugate gradient backpropagation.

Figure 17. Training performance for the BFGS quasi-Newton backpropagation.

Figure 18. Training performance for the Powell-Beale conjugate gradient backpropagation.

Figure 19. Training performance for the Fletcher-Powell conjugate gradient backpropagation.

Figure 20. Training performance for the Levenberg-Marquardt backpropagation.

Figure 21. Training performance for the One step secant backpropagation.

Figure 22. Training performance for the Resilient backpropagation.

Figure 23. Training performance for the Scaled conjugate gradient backpropagation.

5. Conclusions

In this study, the pull-out strength capacity has been observed to increase with increasing diameters. An ANN prediction model for pull-out capacity of chemical anchors embedded into concrete was devised. From this laboratory and computer work the following conclusions were made:

- A significant change observed in pull-out capacity of the specimens with increasing embedment depth. Pull-out strength of the specimens increases with an increasing the depths of hole and there is a notable reduction in pull-out strength of the specimens when embedment diameter decrease from 26 mm to 20 mm.
- The rebar specimen has 14 mm diameter and 180 mm embedment depth showed pull-out strength performance 18.54 % more than 150 mm embedment depth. Moreover, the specimen has 16 mm rebar diameter and 200 mm embedment depth increased pull-out strength performance 18.37 % more than 160 mm embedment depth. Furthermore, the rebar specimen has 18 mm diameter and 220 mm embedment depth improved pull-out strength performance 11.69 % more than 180 mm embedment depth.
- All of R^2 values show that the proposed ANN models are suitable and can predict collapse load of concrete of the experimental values.
- The best algorithm for collapse load of concrete is the Levenberg-Marquardt backpropagation with R^2 of 0.9837.

6. References

[1] Cook RA, Doerr GT, Klingner RE. Bond stress model for design of adhesive anchors. ACI Struct J 1993;90:514–24.

[2] Eligehausen R, Cook RA, Appl J. Behavior and design adhesive bonded anchors. ACI Struct J 2006;103:822-31.

[3] Çaliskan Ö, Yılmaz S, Kaplan H, Kıraç N. Shear strength of epoxy anchors embedded into low strength concrete. Construction and Building Materials 2013;38:723-730.

[4] Cook RA, Collins DM, Klingner RE, Polyzois D. Load–deflection behavior of castin-place and retrofit concrete anchors. ACI Struct J 1992;89:639–49.

[5] Cook RA, Konz RC. Factors influencing bond strength of adhesive anchors. ACI Struct J 2001;98:76–86.

[6] Eligehausen R, Cook RA, Appl J. Behavior and design adhesive bonded anchors. ACI Struct J 2006;103:822–31.

[7] Wu Z, Yang S, Hu X, Zheng J. Analytical Method for Pull-out of Anchor from Anchor-Mortar-Concrete Anchorage System due to Shear Failure of Mortar. Journal of Engineering Mechanics 2007;133(12):1352-1369.

[8] Sakla S.S. S, Ashour FA. Prediction of tensile capacity of single adhesive anchors using neural networks, Computers & Structures, 2005;(83):1792-1803.

[9] Golafshani EM, Rahai A, Sebt MH, Akbarpour H. Prediction of bond strength of spliced steel bars in concrete using artificial neural network and fuzzy logic. Construction and Building Materials 2012;36:411-418.

[10] Tepfers RA. Theory of bond applied to overlapped tensile reinforcement Splices for deformed bars. Division of concrete structures, vol. 73(2). Goteborg: Chalmers. University of Technology; 1973, p. 328.

[11] Bajer M, Bamat J. The glue-concrete interface of bonded anchors. Construction and Building Materials 2012;34:267-274.

[12] Delhomme F, Debicki G, Chaib Z. Experimental behaviour of anchor bolts under pullout and relaxation tests. Construction and Building Materials 2010;24(3):266-274.

[13] Li YJ, Eligehausen R, Ozbolt J, Lehr B. Numerical analysis of quadruple fastenings with bonded anchors. ACI Struct J 2002;99(2):149-56.

[14] James RW, De la Guardia C, McCreary CRJ. Strength of epoxy-grouted anchor bolts in concrete. J Struct Engng 1987;113(12):2365-81.

[15] Bickel TS, Shaikh AF. Shear strength of adhesive anchors. PCI J 2002;47(5):92-101.

[16] Beard MD, Lowe MJS, Cawley P. Ultrasonic guided waves for inspection of grouted anchors and bolts. J Mater Civil Engng 2003;15(3):212-8.

[17] Xu C, Heping C, Bin L, Fangfang Z. Modeling of anchor bolt pullout in concrete based on a heterogeneous assumption. Nuclear Engineering and Design 2011;(241:5): 1345-1351.

[18] Hanbay D, Turkoglu I, Demir Y. An expert system based on wavelet decomposition and neural network for modeling chua's circuit. Expert Systems with Applications 2008; 34: 2278-83.

[19] Haykin S. Neural networks, a comprehensive foundation, College Publishing Comp. Inc 1994.

[20] Topçu IB, Karakurt C, Saridemir M. Predicting the strength development of cements produced with different pozzolans by neural network and fuzzy logic. Materials and Design 2008;29:1986-1991.

[21] Topçu IB, Saridemir M. Prediction of rubberized concrete properties using artificial neural networks and fuzzy logic. Construction & Building Materials 2008;22:532-540.

[22] Topçu IB, Saridemir M. Prediction of compressive strength of concrete containing fly ash using artificial neural networks and fuzzy logic. Computational Materials and Science 2008;41:305-311.

[23] Topçu IB, Saridemir M. Prediction of mechanical properties of recycled aggregate concretes containing silica fume using artificial neural networks and fuzzy logic. Computational Materials and Science 2008;42:74-82.

[24] Topçu IB, Saridemir M. Prediction of rubberized mortar properties using artificial neural network and fuzzy logic. Journal of Materials Processing Technology 2008;199(1-3):108-118.

[25] Topçu IB, Saridemir M. Prediction of properties of waste AAC aggregate concrete using artificial neural networks. Computational Materials and Science 2007;41(1):117-125.

[26] Saridemir M, Topçu IB, Özcan F, Severcan MH. Prediction of long-term effects of GGBFS on compressive strength of concrete by artificial neural networks and fuzzy logic. Construction and Building Materials 2009;23(3):1279-1286.

[27] Hanbay D, Turkoglu I, Demir Y. Prediction of wastewater treatment plant performance based on wavelet packet decomposition and neural networks. Expert Systems with Applications 2008; 34: 1038-1043.

[28] Bilim C, Atiş CD, Tanyildizi H, Karahan O. Predicting the compressive strength of ground granulated blast furnace slag concrete using artificial neural network. Advances in Engineering Software 2009; 40: 334-340.

[29] Nazari A, Riahi S. Computer-aided design of the effects of Fe_2O_3 nanoparticles on split tensile strength and water permeability of high strength concrete. Materials and Design 2011: 32: 3966–3979.

[30] Özcan F. Gene expression programming based formulations for splitting tensile strength of concrete. Construction and Building Materials 2012; 26: 404-410.

[31] Sobhani J, Najimi M, Pourkhorshidi AR, Parhizkar T. Prediction of the compressive strength of no-slump concrete: A comparative study of regression, neural network and ANFIS models. Construction and Building Materials 2010; 24: 709-718.

[32] Erdem H. Prediction of the moment capacity of reinforced concrete slabs in fire using artificial neural networks. Advances in Engineering Software 2010; 41: 270-276.

[33] Uysal M, Tanyildizi H. Predicting the core compressive strength of self-compacting concrete (SCC) mixtures with mineral additives using artificial neural network. Construction and Building Materials 2011;25:4105-4111.

Table 1. Anchor depth, anchor diameter and rebar diameter of the specimens.

Group Number	Rebar Diameter	Anchor Diameter	Anchor Depth
	(mm)	(mm)	(mm)
M1	14	20	140
M2	14	20	150
M3	14	20	160
M4	14	20	170
M5	14	20	180
M6	14	22	140

M7	14	22	150
M8	14	22	160
M9	14	22	170
M10	14	22	180
M11	16	22	160
M12	16	22	170
M13	16	22	180
M14	16	22	190
M15	16	22	200
M16	16	24	160
M17	16	24	170
M18	16	24	180
M19	16	24	190
M20	16	24	200
M21	18	24	180
M22	18	24	190
M23	18	24	200
M24	18	24	210
M25	18	24	220
M26	18	26	180
M27	18	26	190
M28	18	26	200
M29	18	26	210
M30	18	26	220

Table 2. Mechanical properties and mix proportions and of the epoxy.

Compressive strength (MPa)	56
Flexural strength (MPa)	16
Modulus of elasticity	3034
Number of component	2
Mixture density (g/cm^3, 20 ^oC)	1.65

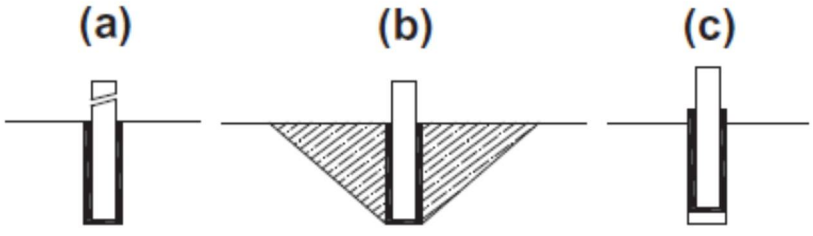

Fig. 1. Separated failure modes used in design methods: (a) tensile failure of the steel anchor bolt, (b) full concrete failure, and (c) bond failure: extraction of the steel bolt from the concrete [11].

(a) (b)

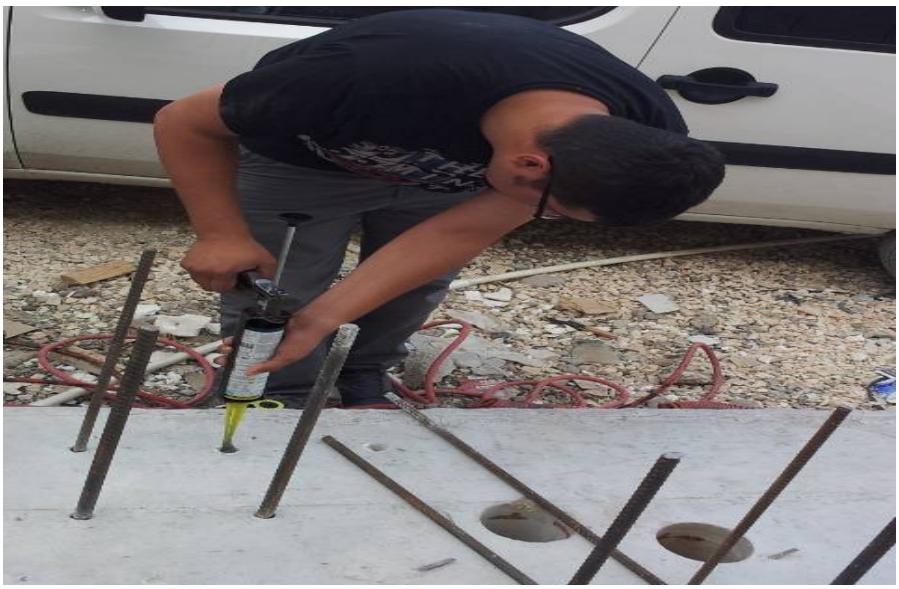

(c)

Fig.2. (a) Drilling, (b) cleaning and (c) embedding of the rebar specimens.

Fig.3. Hydraulic test apparatus of anchor rebar.

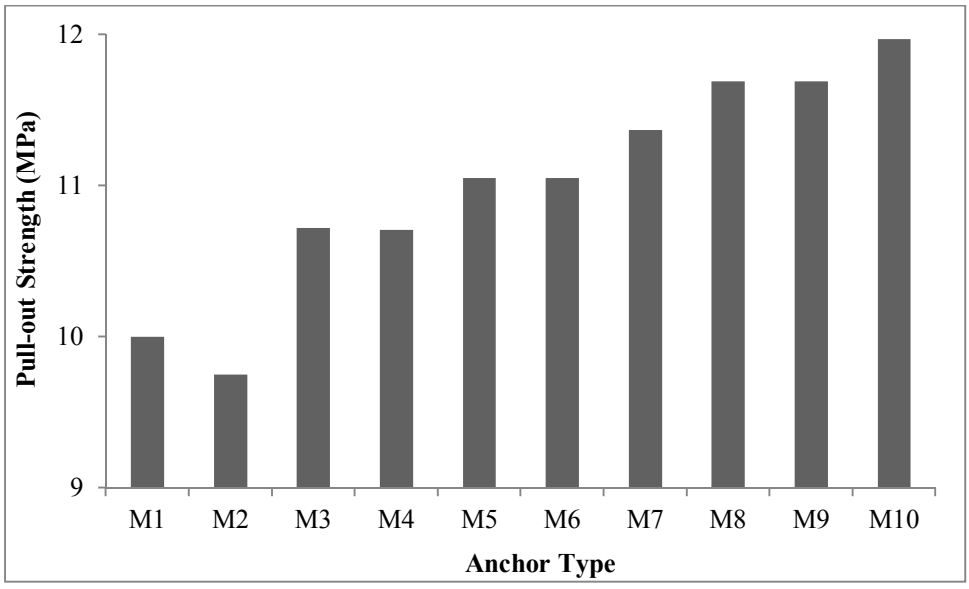

Fig.4. Test results of pull-out strength of the specimens have 14 mm rebar diameter.

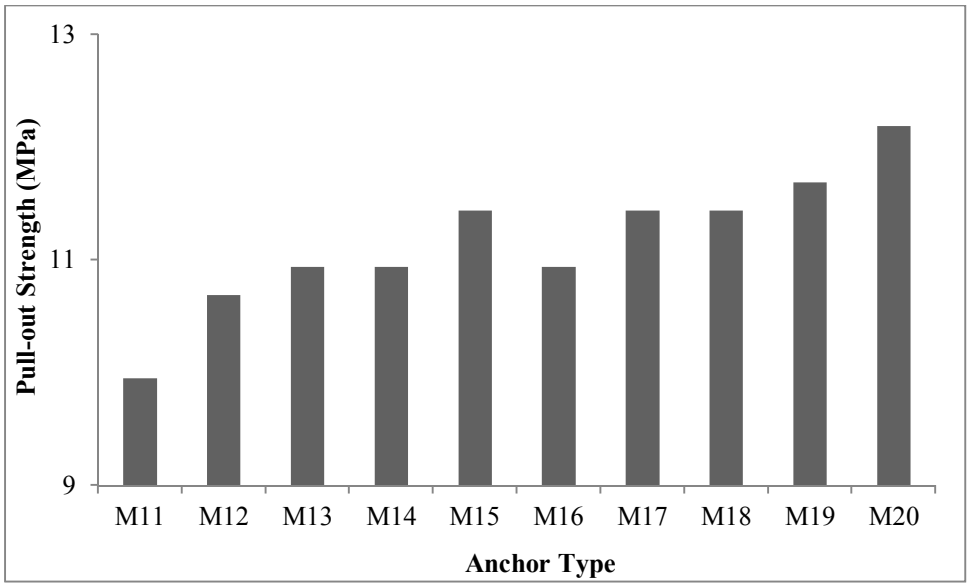

Fig.5. Test results of pull-out strength of the specimens have 16 mm rebar diameter.

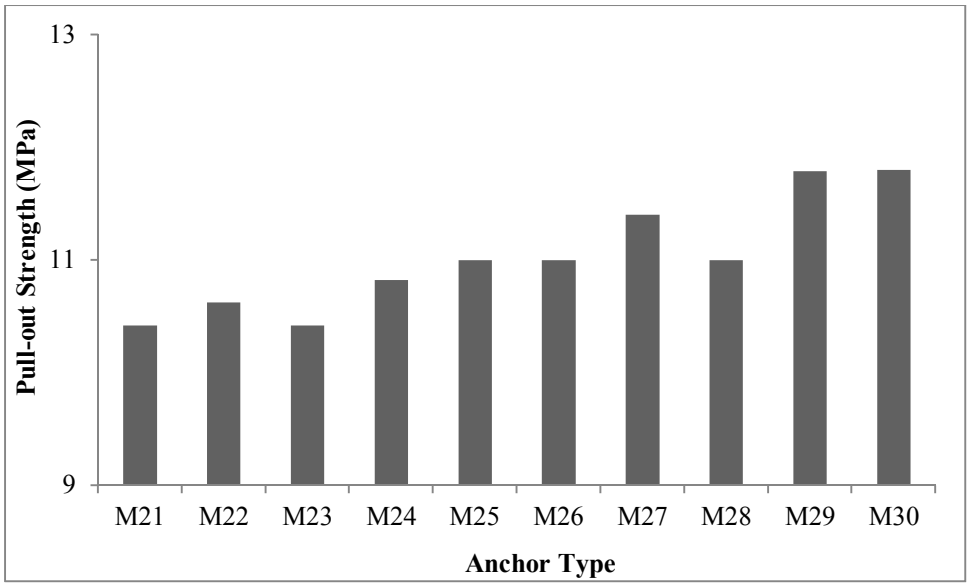

Fig.6. Test results of pull-out strength of the specimens have 18 mm rebar diameter.

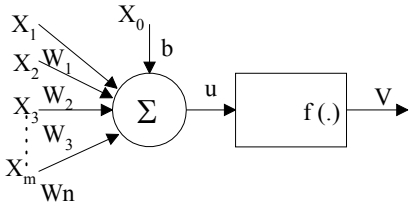

Fig. 7. Artificial neuron model

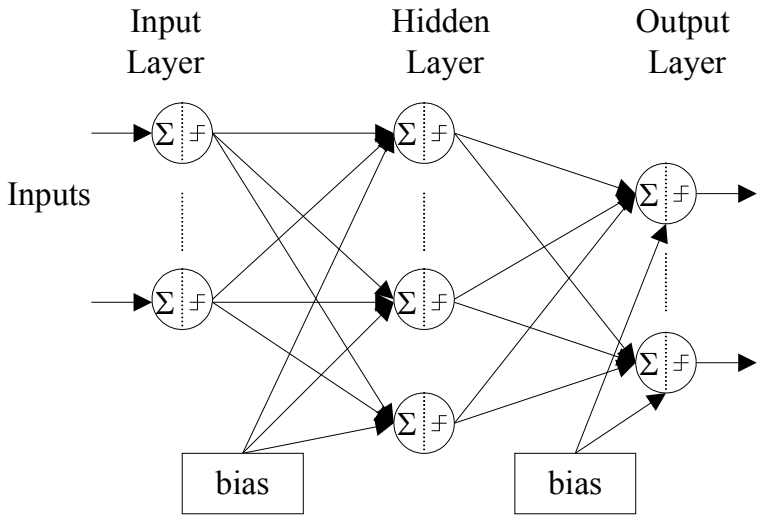

Fig. 8. Multilayer feed forward neural network structure.

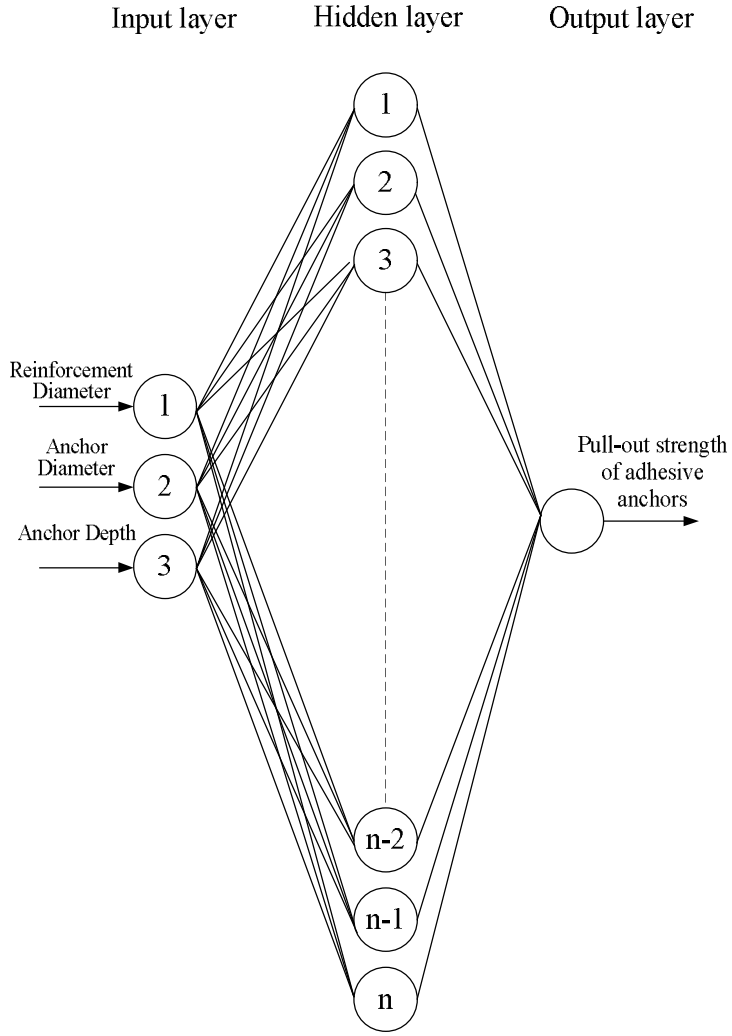

Fig. 9. ANN architecture.

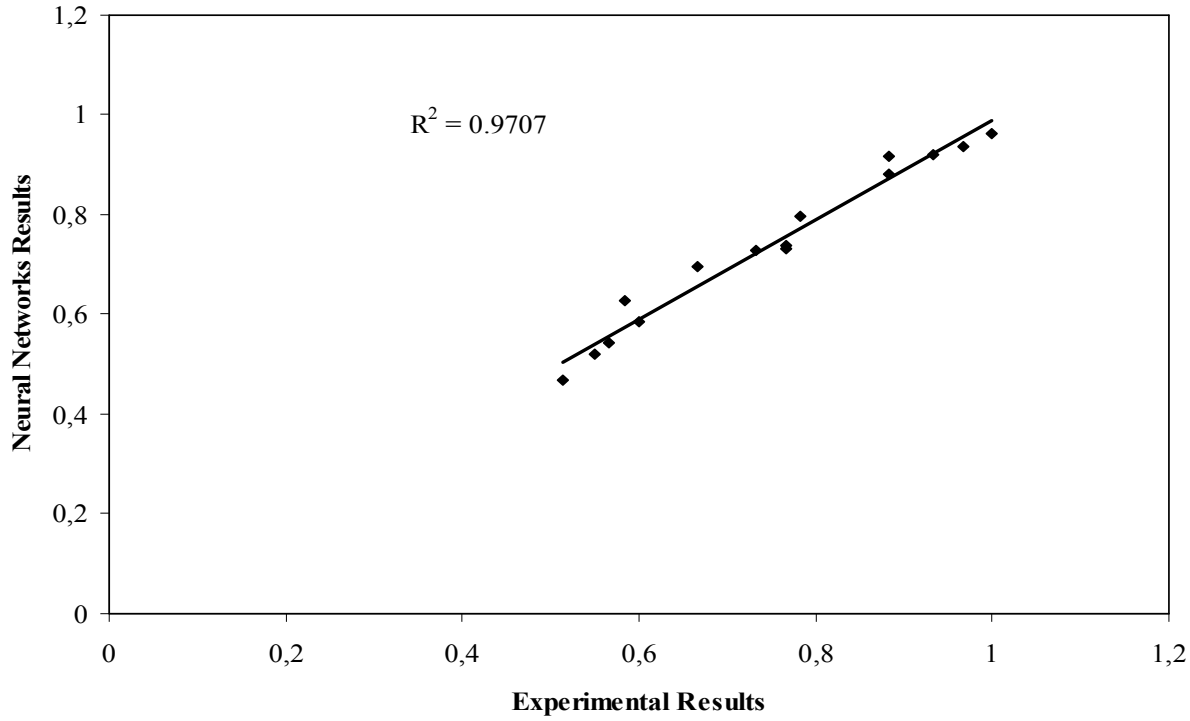

Fig. 10. Linear relationship between measured and predicted compressive strengths for the BFGS quasi-Newton backpropagation.

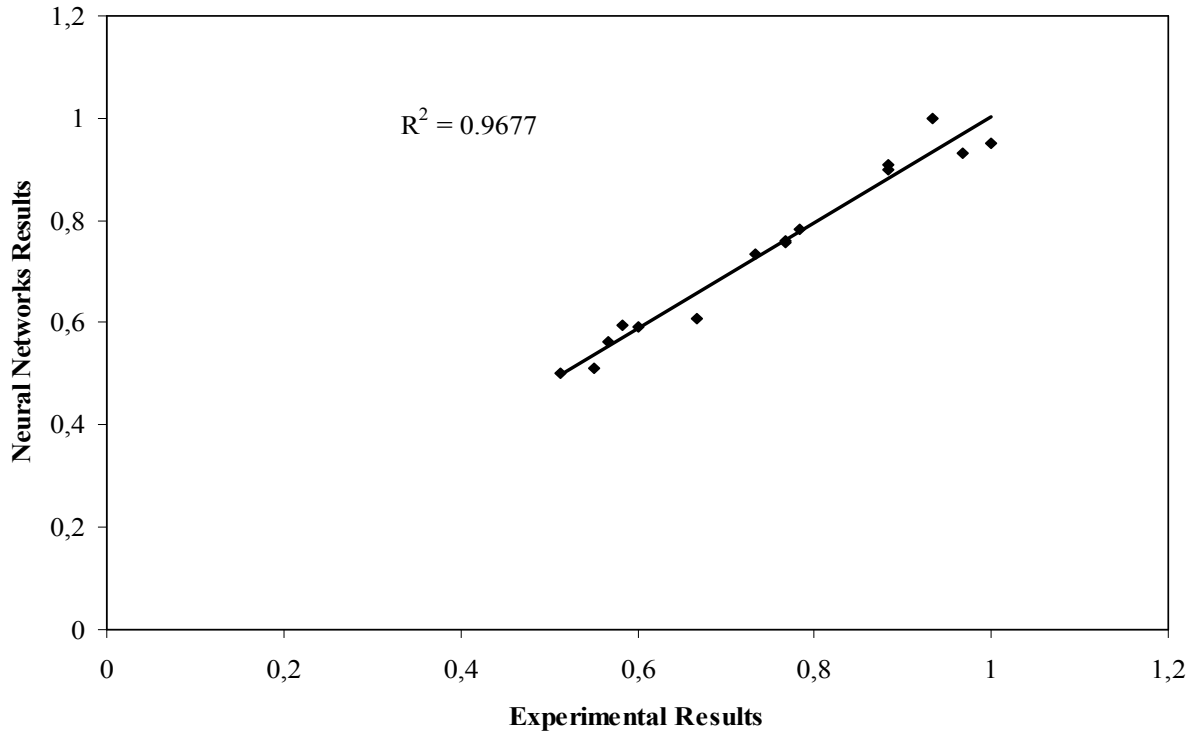

Fig. 11. Linear relationship between measured and predicted splitting tensile strengths for the Powell-Beale conjugate gradient backpropagation.

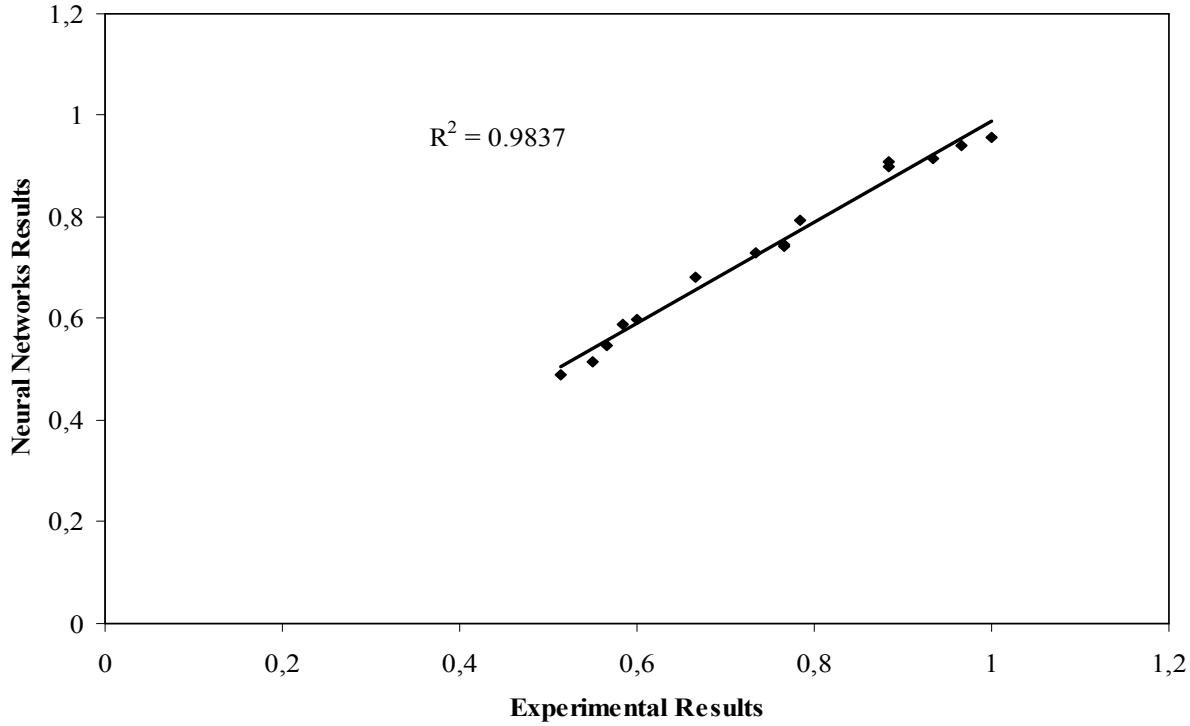

Fig. 12. Linear relationship between measured and predicted compressive strengths for the Levenberg-Marquardt backpropagation.

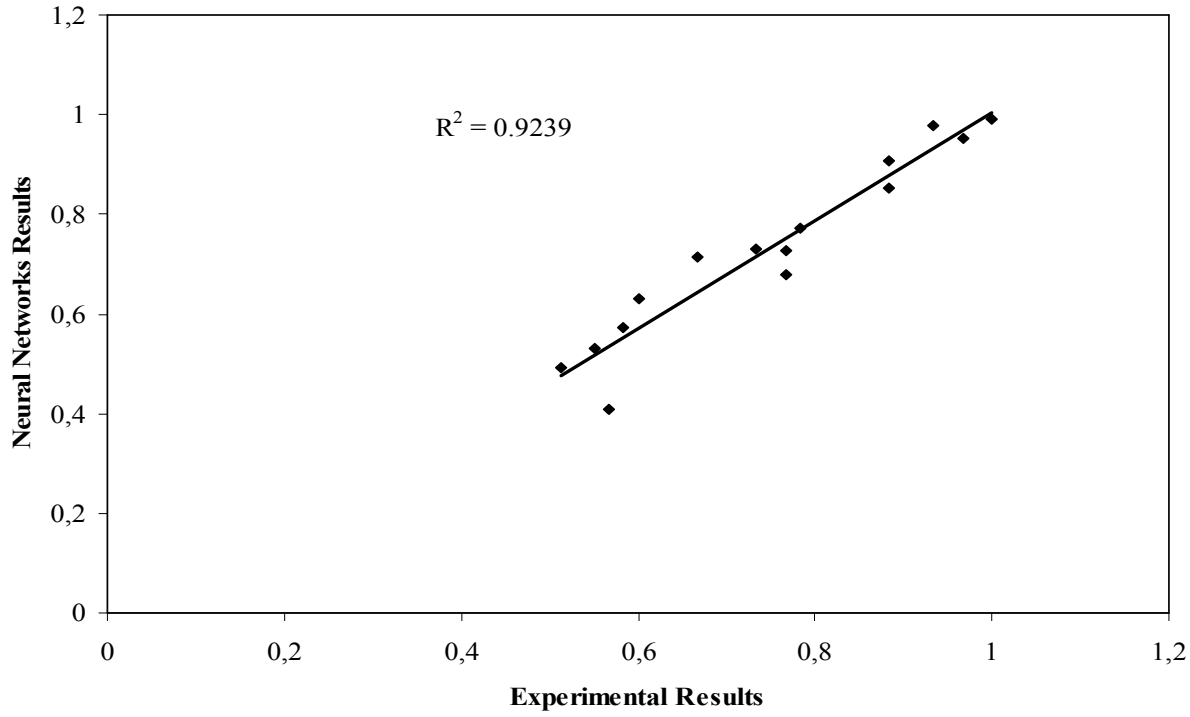

Figure 13. Linear relationship between measured and predicted compressive strengths for the Fletcher-Powell conjugate gradient backpropagation.

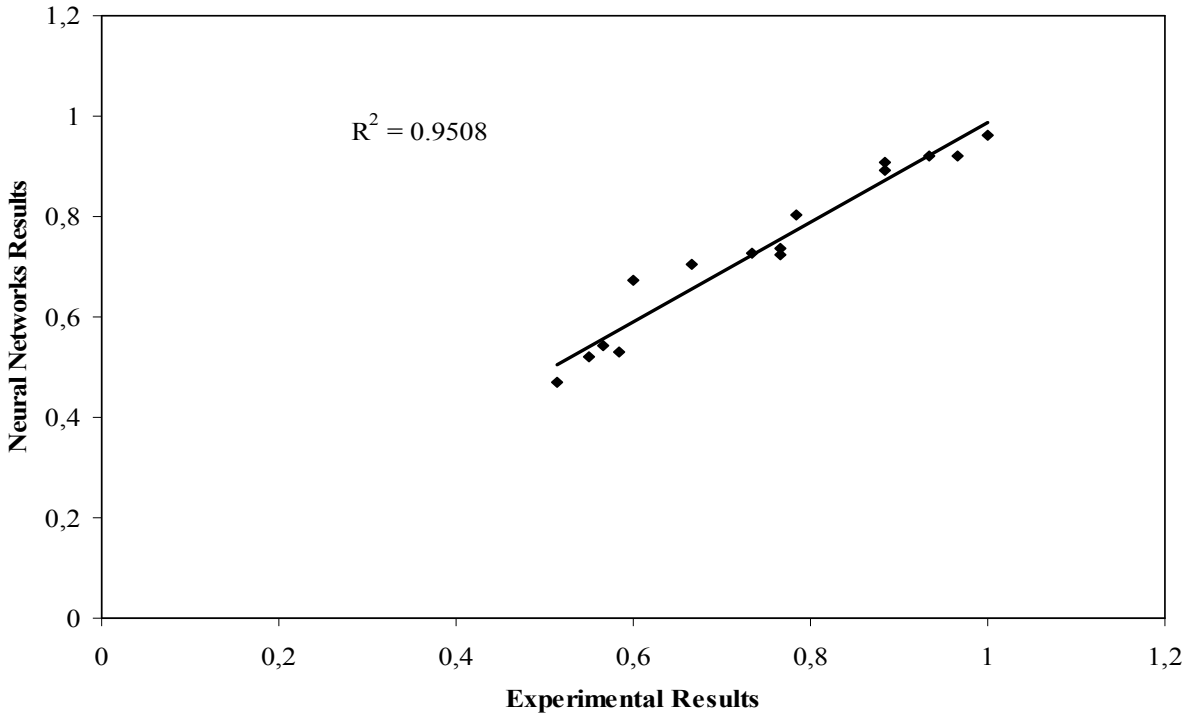

Fig. 14. Linear relationship between measured and predicted splitting tensile strengths for the One step secant backpropagation.

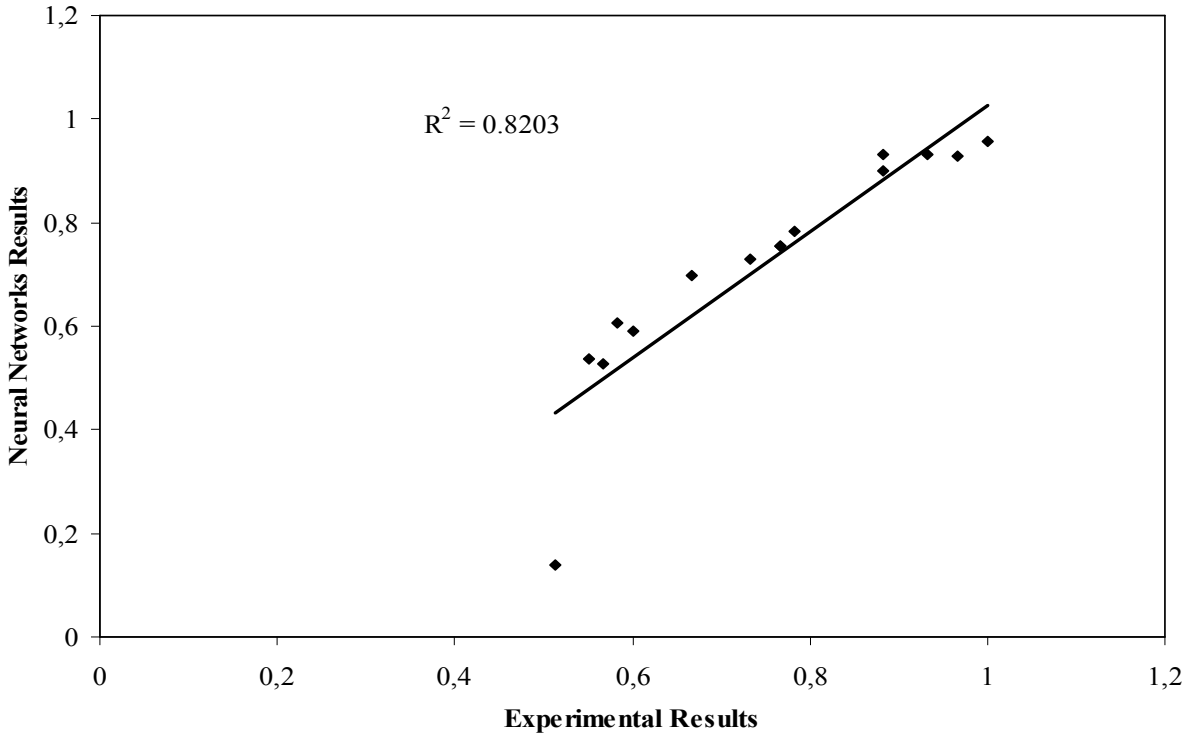

Fig. 15. Linear relationship between measured and predicted compressive strengths for the Resilient backpropagation.

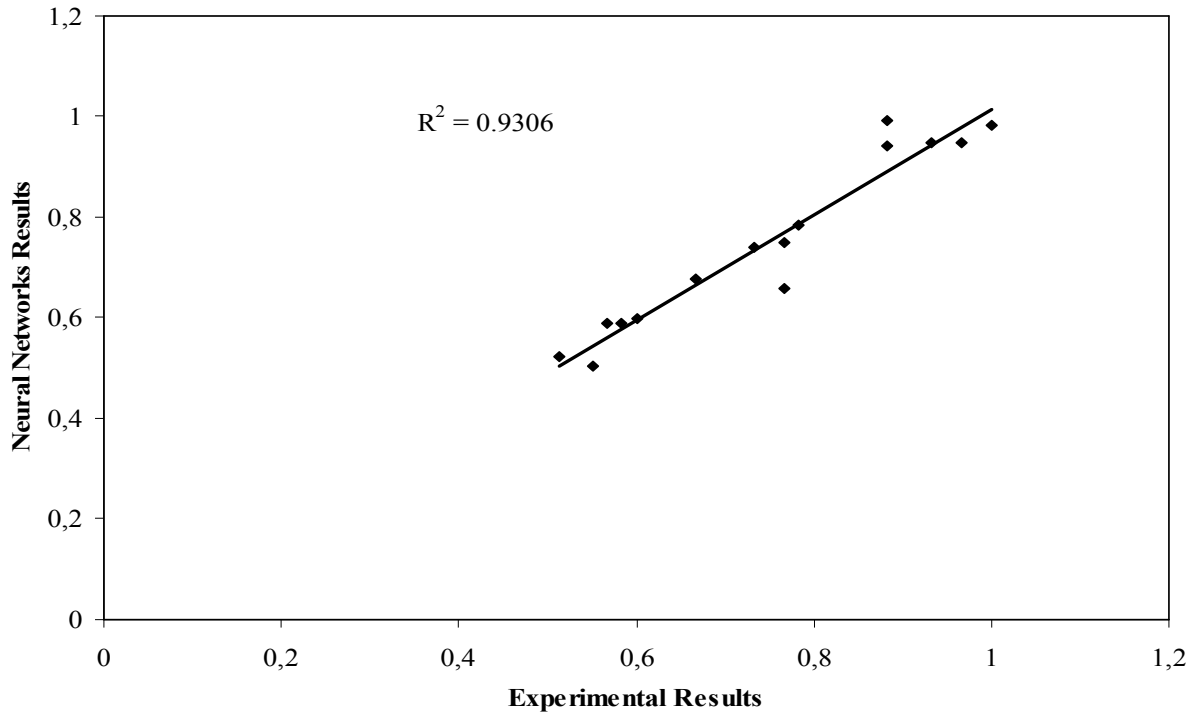

Fig. 16. Linear relationship between measured and predicted splitting tensile strengths for the the Scaled conjugate gradient backpropagation.

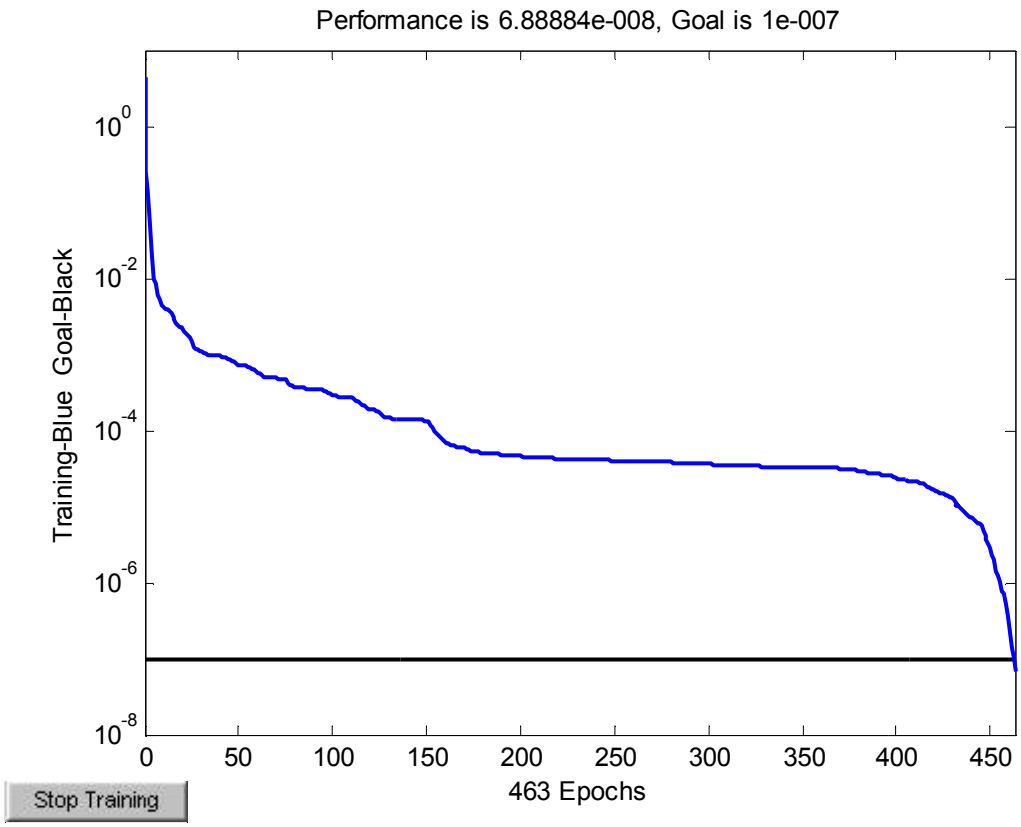

Figure 17. Training performance for the BFGS quasi-Newton backpropagation.

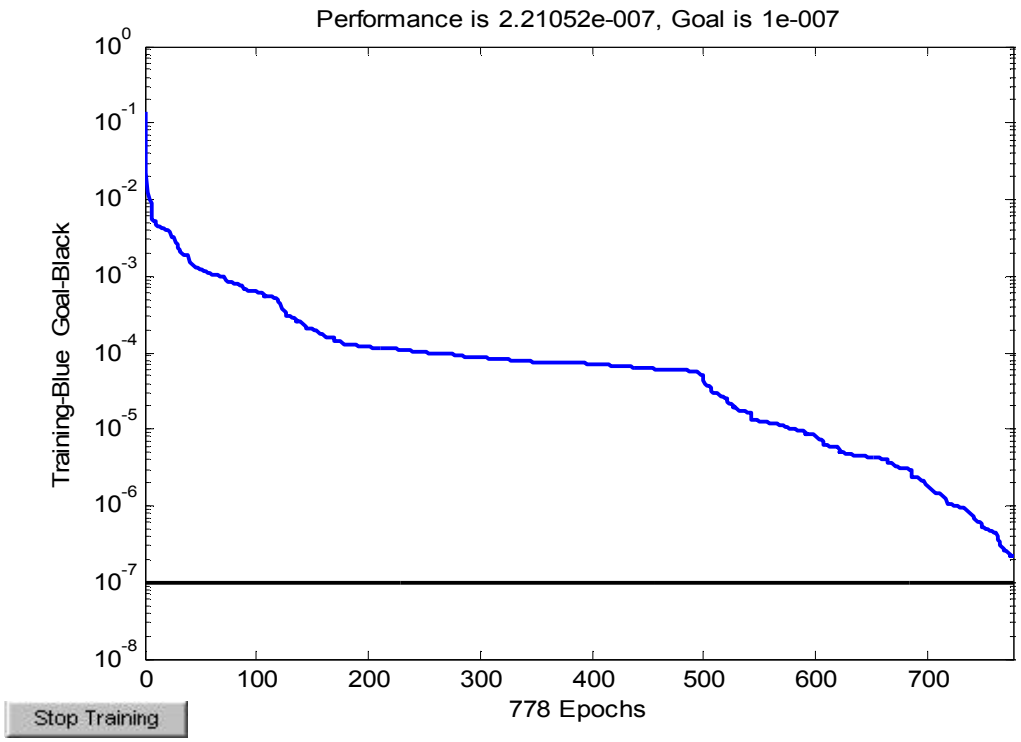

Figure 18. Training performance for the Powell-Beale conjugate gradient backpropagation.

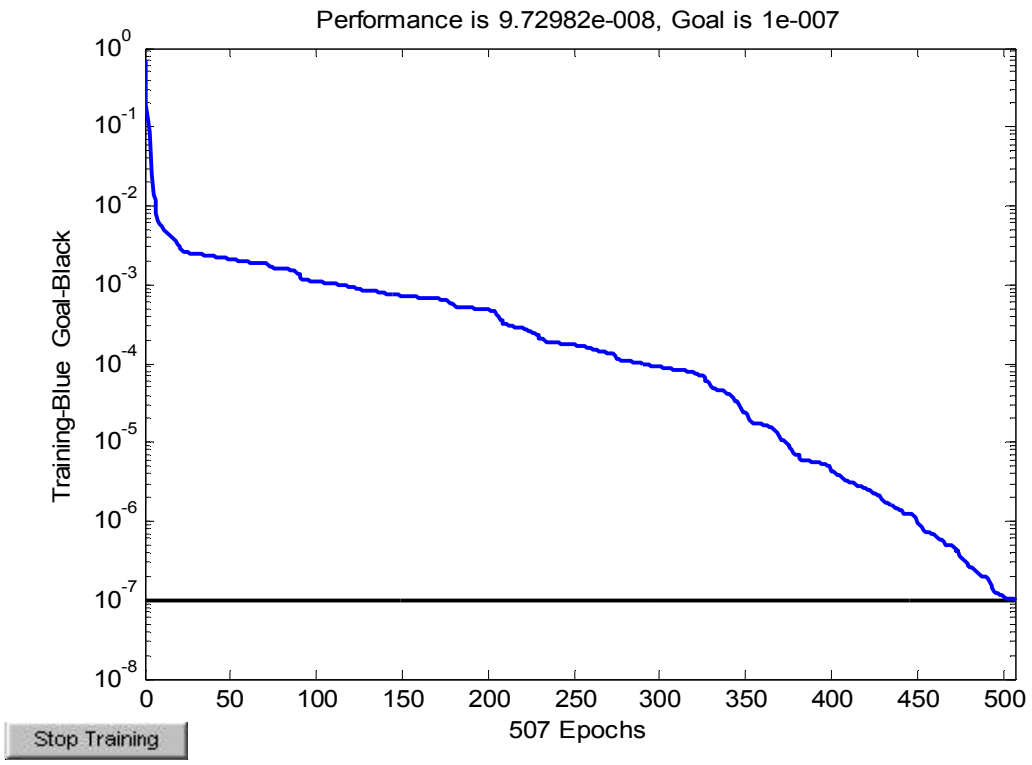

Figure 19. Training performance for the Fletcher-Powell conjugate gradient backpropagation.

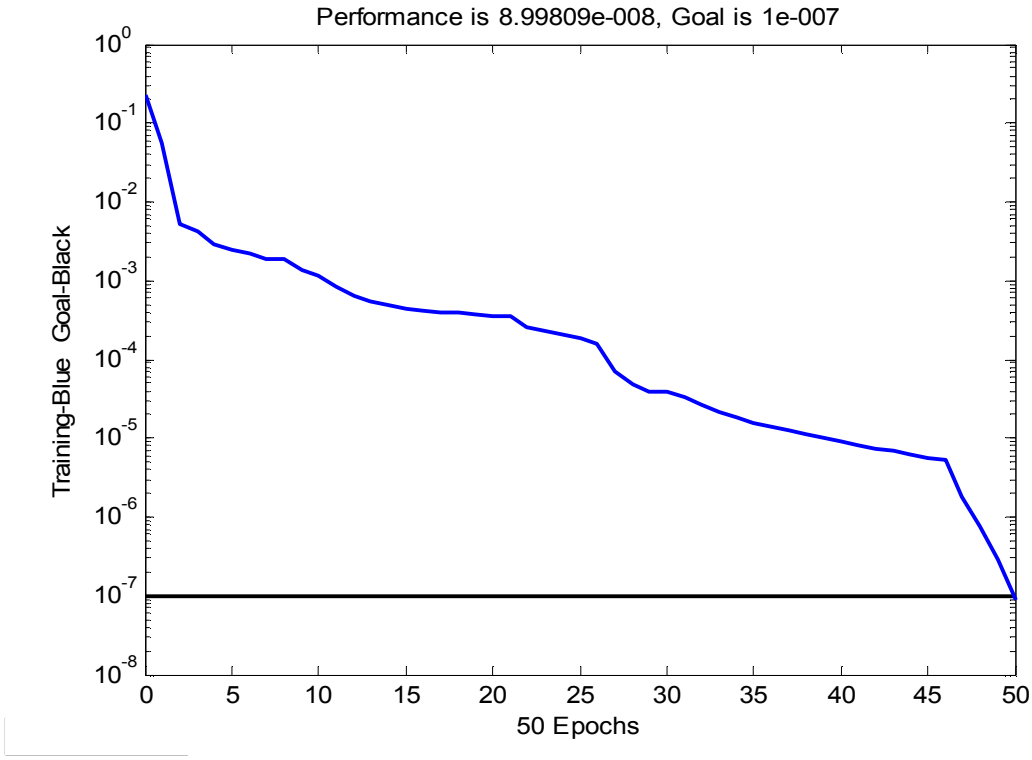

Figure 20. Training performance for the Levenberg-Marquardt backpropagation.

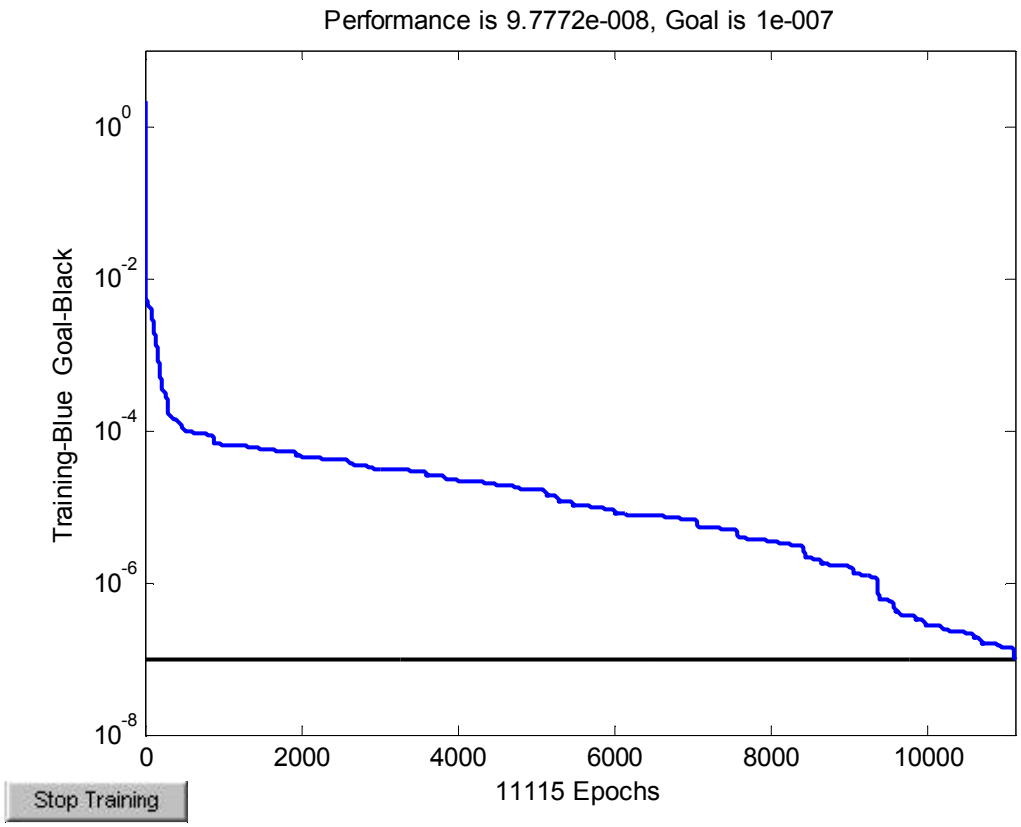

Figure 21. Training performance for the One step secant backpropagation.

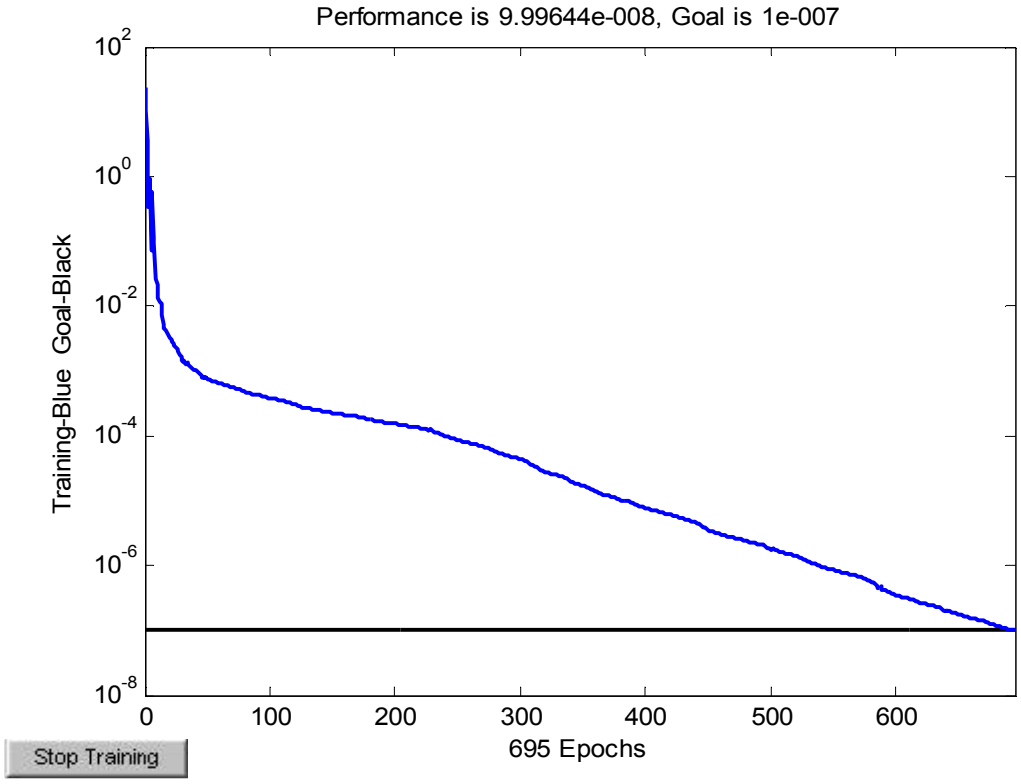

Figure 22. Training performance for the Resilient backpropagation.

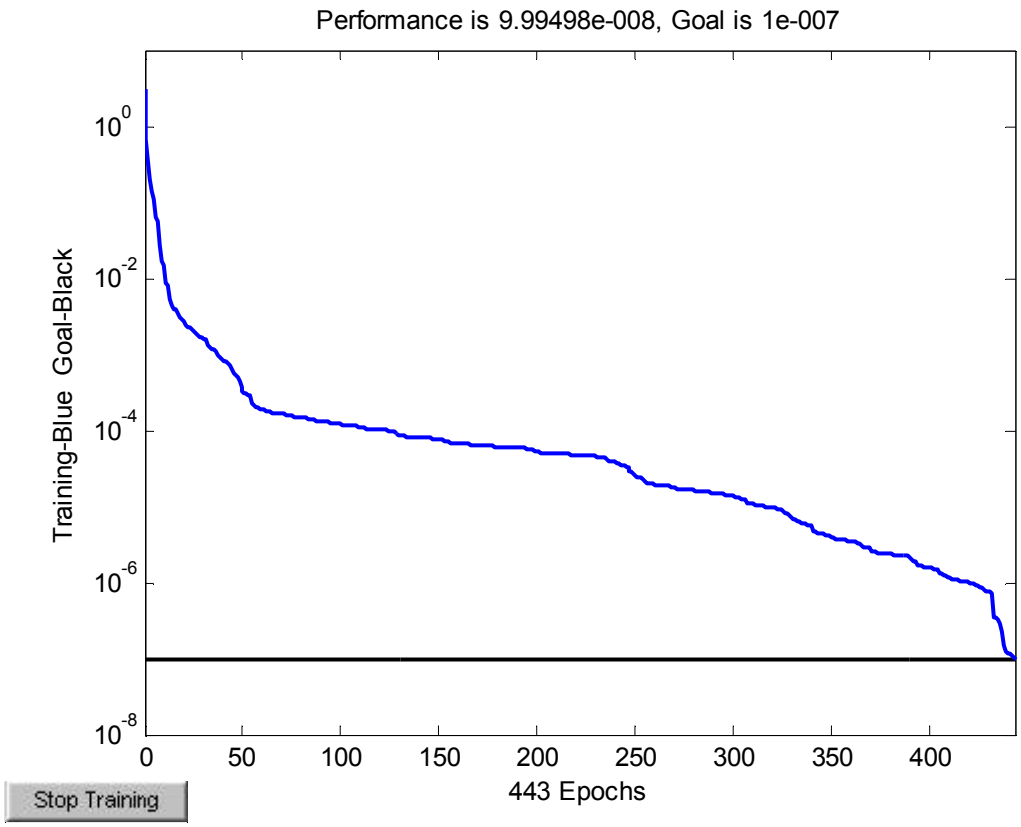

Figure 23. Training performance for the Scaled conjugate gradient backpropagation.